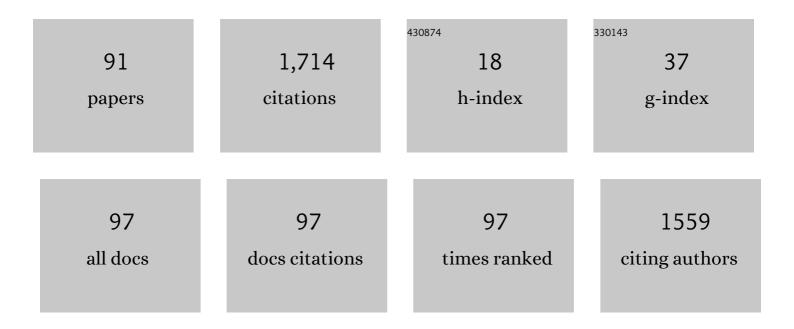
Tomoaki Hori

List of Publications by Year in descending order

Source: https://exaly.com/author-pdf/1653840/publications.pdf Version: 2024-02-01



#	Article	IF	CITATIONS
1	Preferential Energization of Lowerâ€Chargeâ€State Heavier Ions in the Nearâ€Earth Magnetotail. Journal of Geophysical Research: Space Physics, 2022, 127, .	2.4	3
2	Flux Enhancements of Fieldâ€Aligned Lowâ€Energy O ⁺ Ion (FALEO) in the Inner Magnetosphere: A Possible Source of Warm Plasma Cloak and Oxygen Torus. Journal of Geophysical Research: Space Physics, 2022, 127, .	2.4	2
3	Simultaneous Observations of EMICâ€Induced Drifting Electron Holes (EDEHs) in the Earth's Radiation Belt by the Arase Satellite, Van Allen Probes, and THEMIS. Geophysical Research Letters, 2022, 49, .	4.0	3
4	Statistical Study of Seasonal and Solar Activity Dependence of Nighttime MSTIDs Occurrence Using the SuperDARN Hokkaido Pair of Radars. Journal of Geophysical Research: Space Physics, 2022, 127, .	2.4	3
5	Statistical Survey of Arase Satellite Data Sets in Conjunction With the Finnish Riometer Network. Journal of Geophysical Research: Space Physics, 2022, 127, .	2.4	1
6	Signatures of Auroral Potential Structure Extending Through the Nearâ€Equatorial Inner Magnetosphere. Geophysical Research Letters, 2022, 49, .	4.0	1
7	Poleward Moving Auroral Arcs and Pc5 Oscillations. Journal of Geophysical Research: Space Physics, 2022, 127, .	2.4	0
8	Collaborative Research Activities of the Arase and Van Allen Probes. Space Science Reviews, 2022, 218, .	8.1	10
9	Active auroral arc powered by accelerated electrons from very high altitudes. Scientific Reports, 2021, 11, 1610.	3.3	6
10	Investigation of Smallâ€6cale Electron Density Irregularities Observed by the Arase and Van Allen Probes Satellites Inside and Outside the Plasmasphere. Journal of Geophysical Research: Space Physics, 2021, 126, e2020JA027917.	2.4	10
11	Multiâ€Event Analysis of Plasma and Field Variations in Source of Stable Auroral Red (SAR) Arcs in Inner Magnetosphere During Nonâ€5tormâ€Time Substorms. Journal of Geophysical Research: Space Physics, 2021, 126, e2020JA029081.	2.4	7
12	Energyâ€Resolved Detection of Precipitating Electrons of 30–100ÂkeV by a Sounding Rocket Associated With Dayside Chorus Waves. Journal of Geophysical Research: Space Physics, 2021, 126, e2020JA028477.	2.4	2
13	Lowâ€Altitude Ion Upflow Observed by EISCAT and its Effects on Supply of Molecular Ions in the Ring Current Detected by Arase (ERG). Journal of Geophysical Research: Space Physics, 2021, 126, e2020JA028951.	2.4	2
14	ISEE_Wave: interactive plasma wave analysis tool. Earth, Planets and Space, 2021, 73, .	2.5	2
15	Evening Side EMIC Waves and Related Proton Precipitation Induced by a Substorm. Journal of Geophysical Research: Space Physics, 2021, 126, e2020JA029091.	2.4	13
16	Contribution of Electron Pressure to Ring Current and Ground Magnetic Depression Using RAM‧CB Simulations and Arase Observations During 7–8 November 2017 Magnetic Storm. Journal of Geophysical Research: Space Physics, 2021, 126, e2021JA029109.	2.4	4
17	Development of remote HF wave receiver in the backlobe direction of the SuperDARN Hokkaido East radar: Initial observations. Polar Science, 2021, 28, 100669.	1.2	0
18	Fieldâ€Aligned Lowâ€Energy O ⁺ Flux Enhancements in the Inner Magnetosphere Observed by Arase. Journal of Geophysical Research: Space Physics, 2021, 126, e2021JA029168.	2.4	6

Τομοακί Ηογι

#	Article	IF	CITATIONS
19	Rocket Observation of Subâ€Relativistic Electrons in the Quiet Dayside Auroral Ionosphere. Journal of Geophysical Research: Space Physics, 2021, 126, e2020JA028633.	2.4	2
20	Characterization and Calibration of Highâ€Energy Electron Instruments Onboard the Arase Satellite. Journal of Geophysical Research: Space Physics, 2021, 126, e2021JA029110.	2.4	2
21	Penetration of MeV electrons into the mesosphere accompanying pulsating aurorae. Scientific Reports, 2021, 11, 13724.	3.3	37
22	Magnetic Field and Energetic Particle Flux Oscillations and Highâ€Frequency Waves Deep in the Inner Magnetosphere During Substorm Dipolarization: ERG Observations. Journal of Geophysical Research: Space Physics, 2021, 126, e2020JA029095.	2.4	2
23	First Simultaneous Observation of a Night Time Mediumâ€5cale Traveling Ionospheric Disturbance From the Ground and a Magnetospheric Satellite. Journal of Geophysical Research: Space Physics, 2021, 126, e2020JA029086.	2.4	3
24	Relative Contribution of ULF Waves and Whistlerâ€mode Chorus to the Radiation Belt Variation during the May 2017 Storm. Journal of Geophysical Research: Space Physics, 2021, 126, e2020JA028972.	2.4	1
25	Role of Ducting in Relativistic Electron Loss by Whistlerâ€Mode Wave Scattering. Journal of Geophysical Research: Space Physics, 2021, 126, e2021JA029851.	2.4	17
26	On the relationship between energy input to the ionosphere and the ion outflow flux under different solar zenith angles. Earth, Planets and Space, 2021, 73, 202.	2.5	5
27	Study of an equatorward detachment of auroral arc from the oval using groundâ€space observations and the BATSâ€Râ€US – CIMI model. Journal of Geophysical Research: Space Physics, 2021, 126, e2020JA029080.	2.4	4
28	Comparative Study of Electric Currents and Energetic Particle Fluxes in a Solar Flare and Earth Magnetospheric Substorm. Astrophysical Journal, 2021, 923, 151.	4.5	5
29	Arase Observation of the Source Region of Auroral Arcs and Diffuse Auroras in the Inner Magnetosphere. Journal of Geophysical Research: Space Physics, 2020, 125, e2019JA027310.	2.4	7
30	Plasma and Field Observations in the Magnetospheric Source Region of a Stable Auroral Red (SAR) Arc by the Arase Satellite on 28 March 2017. Journal of Geophysical Research: Space Physics, 2020, 125, e2020JA028068.	2.4	8
31	A framework for estimating spherical vector fields using localized basis functions and its application to SuperDARN data processing. Earth, Planets and Space, 2020, 72, .	2.5	4
32	Statistical Properties of Molecular Ions in the Ring Current Observed by the Arase (ERG) Satellite. Geophysical Research Letters, 2019, 46, 8643-8651.	4.0	8
33	Correction to: Review of the accomplishments of mid-latitude Super Dual Auroral Radar Network (SuperDARN) HF radars. Progress in Earth and Planetary Science, 2019, 6, .	3.0	Ο
34	Meridional Distribution of Middleâ€Energy Protons and Pressureâ€Driven Currents in the Nightside Inner Magnetosphere: Arase Observations. Journal of Geophysical Research: Space Physics, 2019, 124, 5719-5733.	2.4	5
35	Remote Detection of Drift Resonance Between Energetic Electrons and Ultralow Frequency Waves: Multisatellite Coordinated Observation by Arase and Van Allen Probes. Geophysical Research Letters, 2019, 46, 11642-11651.	4.0	16
36	Cusp and Nightside Auroral Sources of O ⁺ in the Plasma Sheet. Journal of Geophysical Research: Space Physics, 2019, 124, 10036-10047.	2.4	10

Τομοακί Ηογι

#	Article	IF	CITATIONS
37	Transient ionization of the mesosphere during auroral breakup: Arase satellite and ground-based conjugate observations at Syowa Station. Earth, Planets and Space, 2019, 71, .	2.5	9
38	ERG observations of drift echoes during a unique period of the satellite mission. Earth, Planets and Space, 2019, 71, .	2.5	0
39	Review of the accomplishments of mid-latitude Super Dual Auroral Radar Network (SuperDARN) HF radars. Progress in Earth and Planetary Science, 2019, 6, .	3.0	114
40	Response of the Ionosphereâ€Plasmasphere Coupling to the September 2017 Storm: What Erodes the Plasmasphere so Severely?. Space Weather, 2019, 17, 861-876.	3.7	25
41	The Space Physics Environment Data Analysis System (SPEDAS). Space Science Reviews, 2019, 215, 9.	8.1	332
42	Strong Diffusion of Energetic Electrons by Equatorial Chorus Waves in the Midnightâ€ŧoâ€Đawn Sector. Geophysical Research Letters, 2019, 46, 12685-12692.	4.0	8
43	The ERG Science Center. Earth, Planets and Space, 2018, 70, .	2.5	124
44	Substormâ€Associated Ionospheric Flow Fluctuations During the 27 March 2017 Magnetic Storm: SuperDARNâ€Arase Conjunction. Geophysical Research Letters, 2018, 45, 9441-9449.	4.0	9
45	Theory, modeling, and integrated studies in the Arase (ERG) project. Earth, Planets and Space, 2018, 70, .	2.5	11
46	SCâ€Associated Electric Field Variations in the Magnetosphere and Ionospheric Convective Flows. Journal of Geophysical Research: Space Physics, 2017, 122, 11,044.	2.4	2
47	Characteristics of Seasonal Variation and Solar Activity Dependence of the Geomagnetic Solar Quiet Daily Variation. Journal of Geophysical Research: Space Physics, 2017, 122, 10,796.	2.4	13
48	Propagation and evolution of electric fields associated with solar wind pressure pulses based on spacecraft and groundâ€based observations. Journal of Geophysical Research: Space Physics, 2017, 122, 8446-8461.	2.4	8
49	Morphologies of omega band auroras. Earth, Planets and Space, 2017, 69, .	2.5	6
50	Ground-based instruments of the PWING project to investigate dynamics of the inner magnetosphere at subauroral latitudes as a part of the ERG-ground coordinated observation network. Earth, Planets and Space, 2017, 69, .	2.5	74
51	Wire Probe Antenna (WPT) and Electric Field Detector (EFD) of Plasma Wave Experiment (PWE) aboard the Arase satellite: specifications and initial evaluation results. Earth, Planets and Space, 2017, 69, .	2.5	49
52	Visualization tool for three-dimensional plasma velocity distributions (ISEE_3D) as a plug-in for SPEDAS. Earth, Planets and Space, 2017, 69, .	2.5	6
53	Experiments using Semantic Web technologies to connect IUGONET, ESPAS and GFZ ISDC data portals. Earth, Planets and Space, 2016, 68, .	2.5	3
54	Occurrence characteristics and lowest speed limit of subauroral polarization stream (SAPS) observed by the SuperDARN Hokkaido East radar. Earth, Planets and Space, 2015, 67, .	2.5	9

Τομοακί Ηογι

#	Article	IF	CITATIONS
55	IMF-By dependence of transient ionospheric flow perturbation associated with sudden impulses: SuperDARN observations. Earth, Planets and Space, 2015, 67, .	2.5	7
56	Omega band pulsating auroras observed onboard THEMIS spacecraft and on the ground. Journal of Geophysical Research: Space Physics, 2015, 120, 5524-5544.	2.4	9
57	Statistical study of auroral fragmentation into patches. Journal of Geophysical Research: Space Physics, 2015, 120, 6207-6217.	2.4	8
58	Approximate forms of daytime ionospheric conductance. Journal of Geophysical Research: Space Physics, 2014, 119, 10,397.	2.4	17
59	Long-term variation in the upper atmosphere as seen in the geomagnetic solar quiet daily variation. Earth, Planets and Space, 2014, 66, .	2.5	18
60	An Interactive Data Language software package to calculate ionospheric conductivity by using numerical models. Computer Physics Communications, 2014, 185, 3398-3405.	7.5	6
61	Auroral fragmentation into patches. Journal of Geophysical Research: Space Physics, 2014, 119, 8249-8261.	2.4	18
62	Interuniversity Upper Atmosphere Global Observation Network (IUGONET) Meta-Database and Analysis Software. Data Science Journal, 2014, 13, PDA37-PDA43.	1.3	6
63	Reduction of the fieldâ€aligned potential drop in the polar cap during large geomagnetic storms. Journal of Geophysical Research: Space Physics, 2013, 118, 4864-4874.	2.4	6
64	Inter-University upper Atmosphere Global Observation Network (IUGONET). Data Science Journal, 2013, 12, WDS179-WDS184.	1.3	32
65	Evolution of negative Slâ€induced ionospheric flows observed by SuperDARN King Salmon HF radar. Journal of Geophysical Research, 2012, 117, .	3.3	8
66	Effect of R2â€FAC development on the ionospheric electric field pattern deduced by a global ionospheric potential solver. Journal of Geophysical Research, 2012, 117, .	3.3	15
67	Magnetospheric responses to the passage of the interplanetary shock on 24 November 2008. Journal of Geophysical Research, 2012, 117, .	3.3	11
68	Photoelectron flows in the polar wind during geomagnetically quiet periods. Journal of Geophysical Research, 2012, 117, .	3.3	26
69	Transport and loss of the inner plasma sheet electrons: THEMIS observations. Journal of Geophysical Research, 2011, 116, .	3.3	15
70	Azimuthal auroral expansion associated with fast flows in the near-Earth plasma sheet: Coordinated observations of the THEMIS all-sky imagers and multiple spacecraft. Journal of Geophysical Research, 2011, 116, n/a-n/a.	3.3	7
71	A powerful tool for browsing quick-look data in solar-terrestrial physics: "Conjunction Event Finder― Earth, Planets and Space, 2011, 63, e1-e4.	2.5	12
72	Propagation of large amplitude ionospheric disturbances with velocity dispersion observed by the SuperDARN Hokkaido radar after the 2011 off the Pacific coast of Tohoku Earthquake. Earth, Planets and Space, 2011, 63, 891-896.	2.5	32

Τομοακί Ηογί

#	Article	IF	CITATIONS
73	Localized electron density enhancements in the high-altitude polar ionosphere and their relationships with storm-enhanced density (SED) plumes and polar tongues of ionization (TOI). Annales Geophysicae, 2011, 29, 367-375.	1.6	6
74	Direct measurements of the Poynting flux associated with convection electric fields in the magnetosphere. Journal of Geophysical Research, 2010, 115, .	3.3	18
75	Preonset time sequence of auroral substorms: Coordinated observations by allâ€sky imagers, satellites, and radars. Journal of Geophysical Research, 2010, 115, .	3.3	51
76	Penetration of the convection and overshielding electric fields to the equatorial ionosphere during a quasiperiodic <i>DP</i> 2 geomagnetic fluctuation event. Journal of Geophysical Research, 2010, 115, .	3.3	55
77	Measurements of geomagnetically induced current in a power grid in Hokkaido, Japan. Space Weather, 2009, 7, .	3.7	65
78	S–M–I COUPLING DURING THE SUPER STORM ON 20–21 NOVEMBER 2003. , 2009, , 237-244.		0
79	Response of largeâ€scale ionospheric convection to substorm expansion onsets: A case study. Journal of Geophysical Research, 2008, 113, .	3.3	16
80	Convection electric field in the near-Earth tail during the super magnetic storm of November 20–21, 2003. Geophysical Research Letters, 2006, 33, .	4.0	5
81	Phase Space Density Analysis of Energy Transport in the Earth's Magnetotail. Space Science Reviews, 2006, 122, 69-80.	8.1	5
82	The Loading-Unloading Process in the Magnetotail During a Prolonged Steady Southward IMF Bz Period. COSPAR Colloquia Series, 2005, , 190-193.	0.2	1
83	Plasma transport from multicomponent approach. Geophysical Research Letters, 2005, 32, .	4.0	8
84	Storm-time convection electric field in the near-Earth plasma sheet. Journal of Geophysical Research, 2005, 110, .	3.3	29
85	Magnetotail behavior during storm time "sawtooth injections― Journal of Geophysical Research, 2004, 109, .	3.3	31
86	A substorm-associated drift echo of energetic protons observed by Geotail: Radial density gradient structure. Geophysical Research Letters, 2003, 30, .	4.0	8
87	Average profile of ion flow and convection electric field in the near-Earth plasma sheet. Geophysical Research Letters, 2000, 27, 1623-1626.	4.0	58
88	Structure of the distant magnetotail and its dependence on the IMF By component: GEOTAIL observations. Advances in Space Research, 1997, 20, 949-959.	2.6	27
89	DEVELOPMENT OF STORM-TIME PROTON TOTAL ENERGY BASED ON MULTIOBSERVATION OF NOAA SATELLITES. , 0, , 105-114.		0
90	The Distant Magnetotail: Its Structure, IMF Dependence, and Thermal Properties. Geophysical Monograph Series, 0, , 1-19.	0.1	32

	Томо	daki Hori		
#	Article	IF	CITATIONS	
91	The Energization and Radiation in Geospace (ERG) Project. Geophysical Monograph Series, 0, , 103-116.	0.1	33	